

Article

Genotoxic and Anatomical Deteriorations Associated with Potentially Toxic Elements Accumulation in Water Hyacinth Grown in Drainage Water Resources

Farahat S. Moghanm ¹, Antar El-Banna ², Mohamed A. El-Esawi ^{3,4,*} ,
Mohamed M. Abdel-Daim ^{5,6} , Ahmed Mosa ⁷ and Khaled A.A. Abdelaal ⁸ 

¹ Soil and Water Department, Faculty of Agriculture, Kafrelsheikh University, Kafr el-sheikh 33516, Egypt; fsaad@yahoo.ca

² Genetics Department, Faculty of Agriculture, Kafrelsheikh University, Kafr el-sheikh 33516, Egypt; antar.elbana@agr.kfs.edu.eg

³ Botany Department, Faculty of Science, Tanta University, Tanta 31527, Egypt

⁴ Sainsbury Laboratory, University of Cambridge, Cambridge CB21LR, UK

⁵ Department of Zoology, College of Science, King Saud University, Riyadh 11451, Saudi Arabia; abdeldaim.m@vet.suez.edu.eg

⁶ Pharmacology Department, Faculty of Veterinary Medicine, Suez Canal University, Ismailia 41522, Egypt

⁷ Soils Department, Faculty of Agriculture, Mansoura University, Mansoura 35516, Egypt; ahmedmosa@mans.edu.eg

⁸ EPCRS Excellence Center, Plant Pathology and Biotechnology Laboratory, Agricultural Botany Department, Faculty of Agriculture, Kafrelsheikh University, Kafr el-Sheikh 33516, Egypt; Khaled.elhaies@gmail.com

* Correspondence: mohamed.elesawi@science.tanta.edu.eg; Tel./Fax: +2-0479102930

Received: 10 January 2020; Accepted: 6 March 2020; Published: 10 March 2020



Abstract: Potentially toxic elements (PTEs)-induced genotoxicity on aquatic plants is still an open question. Herein, a single clone from a population of water hyacinth covering a large distribution area of Nile River (freshwater) was transplanted in two drainage water resources to explore the hazardous effect of PTEs on molecular, biochemical and anatomical characters of plants compared to those grown in freshwater. Inductivity Coupled Plasma (ICP) analysis indicated that PTEs concentrations in water resources were relatively low in most cases. However, the high tendency of water hyacinth to bio-accumulate and bio-magnify PTEs maximized their concentrations in plant samples (roots in particular). A Random Amplified Polymorphic DNA (RAPD) assay showed the genotoxic effects of PTEs on plants grown in drainage water. PTEs accumulation caused substantial alterations in DNA profiles including the presence or absence of certain bands and even the appearance of new bands. Plants grown in drainage water exhibited several mutations on the electrophoretic profiles and banding pattern of total protein, especially proteins isolated from roots. Several anatomical deteriorations were observed on PTEs-stressed plants including reductions in the thickness of epidermis, cortex and endodermis as well as vascular cylinder diameter. The research findings of this investigation may provide some new insights regarding molecular, biochemical and anatomical responses of water hyacinth grown in drainage water resources.

Keywords: water hyacinth; potentially toxic elements; genotoxicity; protein patterns; anatomical characters

1. Introduction

The fast global discharge of potentially toxic elements (PTEs) into the hydrosphere has attracted serious focus due to their high bioavailability, bioaccumulation, and biomagnification potentials [1–3].

The consumption of aquatic products is the main pathway of PTEs accumulation in the human body [4]. Some of PTEs such as cadmium (Cd), lead (Pb), arsenic (As), mercury (Hg) and chromium (Cr) have several toxic effects even at low concentrations including series of cancers, anemia, heart attacks, embryotoxicity, neurotoxicity and weakness in the immune system [5]. Therefore, the maximum permissible limits of these elements have been set by the World Health Organization (WHO) to ensure that zero or only the threshold limits of trace levels (part per billion, ppb) are allowed in a water resource [6].

On the other hand, PTEs have several phytotoxic effects on plants by targeting central molecules and vital processes in cells [7]. In this regard, biochemical disorders are the early responses associated with these phytotoxic effects, including enzymes deactivation and several oxidative stress responses linked to the over-production of reactive oxygen species (ROS) [8–10]. According to Jalmi et al. [11], the responses of plant against these early phytotoxic effects are shown in intricate signaling networks functioning in plant cells (e.g., calcium, hormone, and mitogen-activated protein kinase signaling). Furthermore, phytotoxicity of PTEs may also cause severe damage to DNA either through modifying the protein structure of enzymes and/or constraining the production of enzymes at the transcription level, which could also lead to chromosomal aberrations in mitotic cells [12–14]. In addition, PTEs phytotoxicity induced several disorders in biochemical and physiological plant systems including disturbance in cell division, cell cycle impairment, disorders in mitochondrial respiration, dysfunctions in synthesis of photosynthetic pigments, alterations in plasma membrane permeability and defects in water status and nutrients uptake [15]. These biochemical and physiological disorders are associated with several malformations in the anatomical and ultrastructural aspects of plant cells and tissues. The electron-microscopic investigation on reed plants (*Phragmites australis* Cav.) grown in heavy metals-polluted soil illustrated substantial ultrastructural alterations in cell membranes and cytoplasmic organelles of root and stem cells [16]. Additionally, ultrastructural investigation of reed plants showed a distortion in epidermis and mesoderm, which inhibited the radial migration of fluids from roots into peripheral parts and constrained the uptake and translocation of nutrients from roots into shoots. Following these biochemical, physiological and anatomical deteriorations, the common morphological symptoms of PTEs phytotoxicity are chlorosis, withering, falling of leaves as well as defects in shoot and root development [17].

Over the classical techniques of water effluent decontamination (e.g., adsorption, ion exchange, precipitation, coagulation-flocculation, and membrane separation), rhizofiltration could be considered as the most efficient and affordable one at relatively low concentrations of PTEs and large quantities of contaminated water resources. This eco-friendly and cost-effective technique involves using aquatic plants to sequester PTEs from contaminated water effluents into their biomass [18]. Water hyacinth (*Eichhornia crassipes*) has received significant attention to clean-up contaminated water effluents due to its hyperaccumulating potentials of PTEs, rapid proliferation, extensive rooting network and high resistance against biotic and abiotic stress conditions [19,20]. In addition, the potential reuse of water hyacinth biomass in several applications (e.g. biofuels production and biosorbents engineering) provides a circular win-win approach for recycling phytoremediation disposals into value-added products [21]. The bioaccumulation factors of Fe, Mn, Zn, Pb, Cu into water hyacinth biomass can reach respectively 8081, 1540, 3663, 3083, and 538, suggesting its hyperaccumulating potentials to PTEs [22]. Smolyakov et al. [23] evaluated the phytoremediation efficiency of Zn ($500 \mu\text{g L}^{-1}$), Cu ($250 \mu\text{g L}^{-1}$), Pb ($250 \mu\text{g L}^{-1}$) and Cd ($50 \mu\text{g L}^{-1}$) by water hyacinth plants. After 8 days, the removal efficiencies of Cu, Pb, Zn, and Cd were respectively 92, 89, 82 and 76%. Another investigation revealed that water hyacinth plant could remove about 99.5% of Cr (VI) from industrial mines wastewater as well as reducing total dissolved solids (~19%), biological oxygen demand (~50%) and chemical oxygen demand (~34%) [24].

Despite intensive research undertaken on wastewater purification using water hyacinth plants, research trials undertaken to improve its adaptability and bioaccumulation potentials to PTEs are still very few. In this regard, studying the genotoxicity of PTEs based on protein profile and DNA

variability has advantageous due to their sensitivity and rapid responses. PTEs-induced phytotoxicity caused significant alterations in leaf protein profiles including reduction of photosynthetic protein and cellular damage at the DNA level and organelles such as mitochondria or lysosomes [25]. In this regard, the behavior of PTEs on biochemical parameters of water hyacinth is contradictory. For instance, the interference of Cd and Mn ions with protein synthesis caused inhibition in RNA and DNA content. However, Zn ions caused the opposite effect through increasing RNA and DNA content and protein synthesis [26]. To the best of the authors' knowledge, molecular and anatomical investigations on water hyacinth plants grown under toxic elements stress are still insufficient. Therefore, the main objectives of this study are to investigate the effect of PTEs contamination on DNA pattern, protein profile characters, and anatomical structure of water hyacinth populations grown in two drainage water resources compared to another population grown in freshwater source (Nile River).

2. Results

2.1. Potentially Toxic Elements Concentration in Water and Water Hyacinth Plants

Elemental analysis of water and plant samples is illustrated in Table 1. In general, elements concentration in drainage water samples was greatly higher than freshwater samples. Ca, Na, Mg, and K showed the highest concentrations in water samples. Concentrations of PTEs in fresh and drainage water samples were relatively low in most cases, and some of these PTEs were below detection limit. Elamom drain recorded the highest Ca, Mg, K, Na, and P levels (3.11, 4.08, 4.74, 8.34, and 8.0-fold of the freshwater source). Arsenic (As) and nickel (Ni) were detected only in Elamom drain. This drain recorded the highest concentrations of Ba, Sr, and V. Concentrations of Ca, Mg, K, Na, and P showed higher values in root and leaf samples, particularly in drainage water sources. These elements showed higher accumulation in leaves than roots suggesting their nutritional functions in plant [27].

Table 1. Concentration of PTEs in water and water hyacinth samples.

Element	Water (mg L ⁻¹)			Plant Roots mg kg ⁻¹			Plant Leaves mg kg ⁻¹		
	A	B	C	A	B	C	A	B	C
Major Elements									
Ca	39.82	49.84	123.95	5115.49	3506.76	3637.54	9368.2	5687.34	9160
Mg	16.06	18.69	65.53	2762.73	1999.23	1761.56	2067.46	2015.32	2924.29
K	6.93	10.29	32.85	10,529.1	3811.48	5475.24	21,437.14	16,600.94	12,658.13
Na	33.33	51.07	278.15	2206.35	2713.04	3062.65	1451.18	5601.7	6519.1
P	0.05	0.02	0.40	1261.99	1982.92	1538.97	1908.3	1628.3	3438.18
Ag	0.001	N.D	N.D	0.48	0.68	0.42	0.61	0.54	1.17
PTEs									
Al	0.0049	0.0087	0.0028	5290.05	12,431.01	2832.28	431.49	520.26	487.33
As	N.D	N.D	0.0054	0.15	1.69	1.71	0.01	N.D	N.D
Ba	0.053	0.06	0.1016	3.00	2.78	3.51	5.98	5.38	6.15
Cd	0.0021	0.0016	N.D	0.26	0.23	0.06	N.D	N.D	N.D
Co	N.D	N.D	N.D	4.47	3.5	3.15	N.D	N.D	N.D
Cr	N.D	N.D	N.D	14.29	33.1	6.85	2.38	2.71	2.57
Cu	0.0036	0.0031	0.0023	22.64	27.14	19.25	17.78	15.5	14.9
Fe	N.D	N.D	N.D	5142.03	8697.08	3285.98	673.4	529.63	589.45
Mn	0.0011	0.0367	0.0013	1489.01	245.98	418.64	149.76	169.63	174.13
Mo	0.0071	N.D	N.D	0.04	0.35	N.D	N.D	N.D	N.D
Ni	N.D	N.D	0.0006	12.84	10.54	6.27	2.93	1.42	1.98
Sb	0.011	0.0092	N.D	1.09	1.38	0.56	0.54	0.12	0.46
Sr	0.3437	0.3782	1.107	40.58	32.89	30.36	59.01	44.98	62.16
Ti	0.0024	0.0007	0.0005	575.53	874.73	324.7	56.41	47.72	54.32
V	0.0096	0.014	0.0174	22.27	36.07	13.7	1.53	1.47	1.61
Zn	0.0056	0.0098	0.0044	31.99	50.31	20.63	16.42	19.37	16.89

A: Fresh water (Nile River), B: Nashart drain, C: Elamom drain and ND means below detection limit.

PTEs showed a high biomagnification potential based on their high concentration in plant organs. Immobile PTEs (e.g., Al, As, Cd, Co, Cr, Cu, Fe, Mn, Mo, Ni, Sb, Ti, V, and Zn) showed higher accumulation in roots; however, mobile PTEs (e.g., Ba and Sr) exhibited higher accumulation in leaves. The bioaccumulation factor (BAF) of PTEs (Al, Ba, Cu, Mn, Sr, V, and Zn) confirmed the hyperaccumulating potentials of water hyacinth (Table 2). According to Ma et al. [28], plants are classified as hyperaccumulators when BAF value is higher than 10.

Table 2. Bioaccumulation factor (BAF) and translocation factor (TF) for the most detected PTEs in water resources.

PTEs	BAF						TF		
	BAF _{roots}			BAF _{leaves}			A	B	C
	A	B	C	A	B	C			
Al	1,079,602.0	1,428,851.7	1,011,528.6	88,059.2	59,800.0	174,046.4	0.082	0.042	0.172
Ba	56.6	46.3	34.5	112.8	89.7	60.5315	1.993	1.935	1.752
Cu	6288.9	8754.8	8369.6	4938.9	5000.0	6478.261	0.785	0.571	0.774
Mn	1,353,645.5	6702.5	322,030.8	136,145.5	4622.1	133,946.2	0.101	0.690	0.416
Sr	118.1	87.0	27.4	171.7	118.9	56.15176	1.454	1.368	2.047
Ti	239,804.2	1,249,614.3	649,400.0	23,504.2	68,171.4	108,640	0.098	0.055	0.167
V	2319.8	2576.4	787.4	159.4	105.0	92.52874	0.069	0.041	0.118
Zn	5712.5	5133.7	4688.6	2932.1	1976.5	3838.636	0.513	0.385	0.819

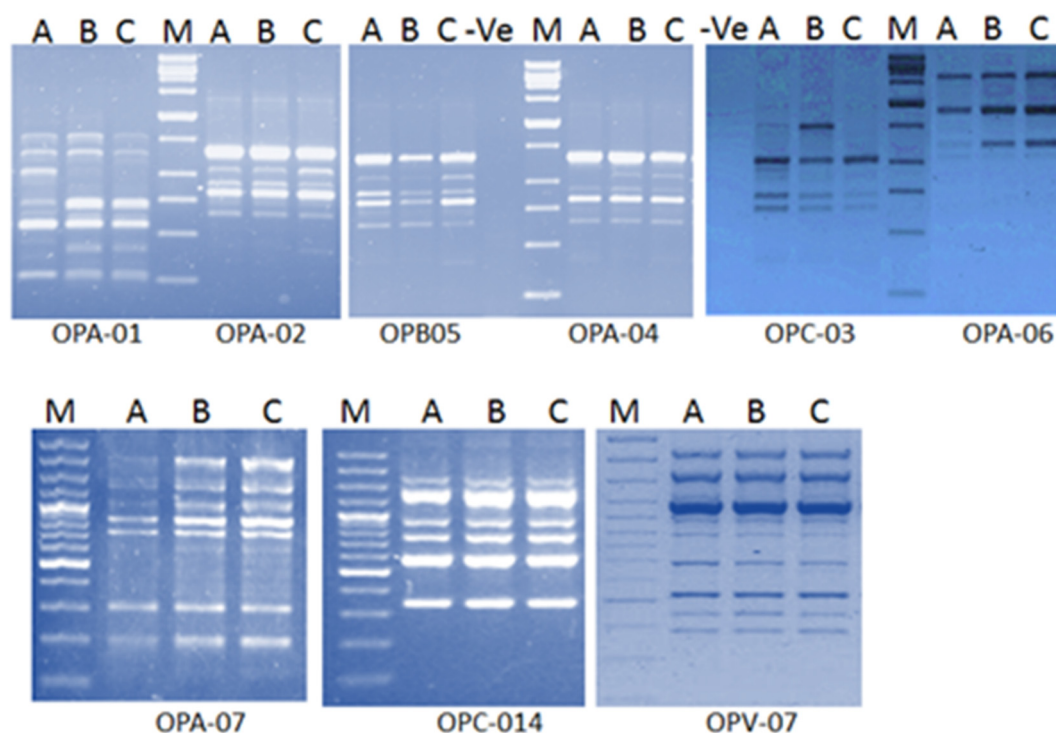
A: Fresh water (Nile River), B: Nashart drain, C: Elamom drain.

2.2. Molecular Analysis

A single clone from a population covering the entire distribution area in Nile River was selected as a source of the studied populations. Nine random primers were used to differentiate among populations grown in fresh and drainage resources (Table 3 and Figure 1). The OPA-01 primer gave 8 different bands sized from 1560 to 250 bp. Two of which were polymorphic bands with 25% polymorphism percentage and the other one was monomorphic. It was clear that the sizes of 100 bp were existed only in the freshwater population and disappeared in other drainage water populations. On the other hand, the band size of 375 bp was existed only in both drainage water populations. The application of OPA-02 primer indicated the amplification of seven bands with a size ranged from 1400 to 375 bp, which one of them was polymorphic with 14.3% polymorphism percentage. The Band with the size of 375 bp was unique and found once in the population of Elamom drain. The OPB-05 primer separated six amplified bands with a size ranging from 1300 to 370 bp. Two of these bands were polymorphic (33.3% polymorphism percentage) and four were monomorphic. The band with a size of 1000 bp was absent in the population of Nashart drain. However, the band with molecular size of 370 bp was unique in the population of Elamom drain. The OPA-04 primer exhibited five different bands ranging from 1450 to 600 bp, where one of them was polymorphic (22% polymorphism percentage). Moreover, it is cleared that the band with a size of 1200 bp was existed only in both populations grown in drainage water resources.

Table 3. Primers, their respective base sequences, number of amplified bands, number of polymorphic bands, and polymorphism percentages for the analyzed plants.

Primer Code	Primer Sequence 5'→3'	No. Polymorphic Bands	Total Bands	Polymorphism %
OPA-01	5'-CAGGCCCTTC-3'	2	8	33.3
OPA-02	5'-TGCCGAGCTG-3'	1	7	16.7
OPB-05	TGCGCCCTTC	2	6	50
OPA-04	5'-AATCGGGCTG-3'	1	5	25
OPC-03	GGGGTCTTT	1	5	25
OPA-06	5'-GGTCCCTGAC-3'	0	4	0.0
OPA-07	5'-GAAACGGGTG-3'	0	7	0.0
OPC-14	5'-TGCGTGCTTG-3'	0	6	0.0
OPV-07	5'-GAAGCCAGCC-3'	0	9	0.0
Total		7	57	

**Figure 1.** RAPD fragment amplified from genomic DNA of Water hyacinth leaves resulted. (M: marker, -ve: negative control (H₂O), A: Nile River, B: Nashrat drain, C: Elamom drain).

The OPC-03 primer separated five different bands with a size ranging from 1500 to 600 bp. One of them was polymorphic (20% polymorphism percentage) and another one with the size of 1500 bp was absent only in the population of Elamom drain. Data presented in Table 2 showed that the nine used RAPD primers produced a total of 57 amplified bands. Among them, five were polymorphic with 12.3% polymorphism percentage. The OPB-05 primer gave the highest total polymorphic bands, whereas OPA-02 primer recorded the lowest ones. Furthermore, the primers OPA-06, OPA-07, OPC-14 and OPV-07 produced only monomorphic bands, and these primers were not able to differentiate among the populations of fresh and drainage water resources.

2.3. Total Protein Analysis by SDS-PAGE

The electrophoretic profiles and banding pattern of total protein isolated from leaves and roots of water hyacinth grown in fresh and drainage water resources are presented in Figure 2 and Table A3. SDS-PAGE banding patterns of leaves revealed 23 bands with different molecular weights. Among them, five bands showed high variability; however, the other 18 bands were commonly detected in the studied populations. Both sources of drainage water caused changes in the protein electrophoretic profiles. These changes include alteration in band intensities (66, 65.8 and 36 KDa) and the appearance of new bands (64.3 and 50.5 KDa). The protein banding pattern of roots revealed higher variation among plants grown either in fresh or drainage water resources compared to the banding pattern of proteins isolated from leaves. SDS-PAGE banding patterns showed 15 scorable bands, where 12 out of them were de novo synthesized in plants grown in drainage water. The most visible alterations in SDS-PAGE patterns of roots were the appearance of new bands with molecular weight of 46, 45.7, 45, 44.4, 36, 29, 28.4, 28, 17.6, 15, 14, and 13.9 and 139 KDa in populations grown in drainage water sources.

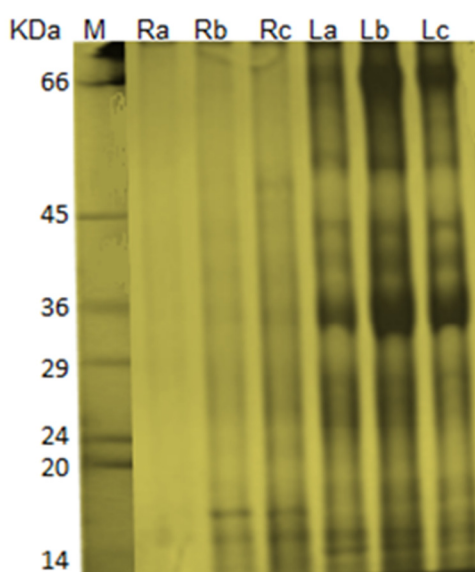


Figure 2. SDS-Polyacrylamide gel electrophoresis showing protein bands patterns of water hyacinth. M: marker (High molecular weight Sigma), R: protein isolated from roots, L: protein isolated from leaves. a: Nile River, b: Nashrat drain, c: Elamom drain).

2.4. Anatomical Structure

The anatomical investigation of water hyacinth plants (roots, leaves, and petioles) in transverse sections is illustrated in Figure 3 and Table 4. It is realized that the epidermis of root, leaf, and petiole consists of one layer of quadrangular cells. Unlike leaf and petiole, root epidermis was not covered by cuticle. Root diameter showed a noticeable reduction in plants grown in drainage water. This reduction was associated with a notable decrease in epidermis, cortex and endodermis thickness as well as vascular cylinder diameter. Additionally, number of metaxylem and diameter of xylem vessels were higher in plants grown in freshwater compared to those grown in drainage water resources (Figure 3A–C and Table 4). Furthermore, epidermis of leaf lamina in transverse section has one layer with very thin cuticle layer, and the mesophyll tissue was distinguished into a palisade and spongy tissue. Substantial reductions in lamina thickness, upper epidermis, lower epidermis and mesophyll tissue thickness as well as length and width of vascular bundles were observed on plants grown in drainage water relative to those grown in freshwater (Figure 3D,F and Table 4).

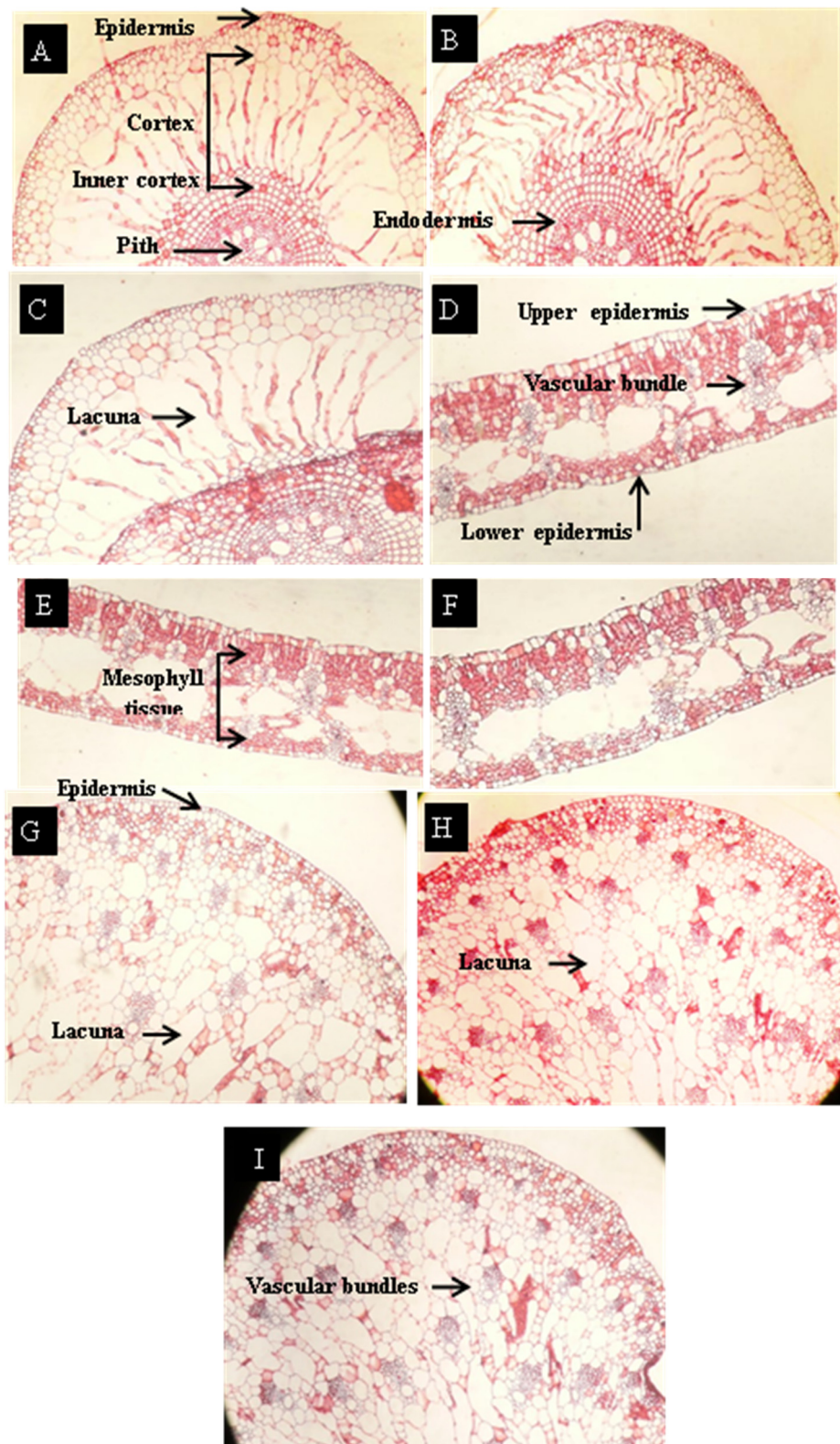


Figure 3. Transverse sections in roots (A–C), leaves (D–F) and petioles (G–I) of *Eichhornia crassipes* (Mart.) Solms. A. Root (Nile River), B. Root (Nashrat drain), C. Root (Elamom drain), D. Lamina (Nile River), E. Lamina (Nashrat drain), F. Lamina (Elamom drain), G. Petiole (Nile River), H. Petiole (Nashrat drain), I. Petiole (Elamom drain).

Table 4. Anatomical characters of roots, leaves and petioles of water hyacinth grown in fresh water (control) and drainage water resources.

Anatomical Characters of Roots	Diameter of Root (μ)	Thickness of Epidermis (μ)	Thickness of Cortex (μ)	Thickness of Endodermis (μ)	Diameter of Vascular Cylinder (μ)	Diameter of Xylem Vessel (μ)	
(Fresh water)	596	4.52	241.39	6.5	182.66	14.26	
Nashrat drain	336.66	2.75	158.61	7.5	148.61	9.65	
Elamom drain	476.20	3.22	210.4	6.29	154	12.43	
Anatomical characters of leaves	Thickness of lamina (μ)	Thickness of upper epidermis (μ)		Thickness of lower epidermis (μ)	Thickness of mesophyll tissue (μ)	Length of vascular bundle (μ)	Width of vascular bundle (μ)
(Fresh water)	164.16	8.26		7.3	148.6	49.9	30.24
Nashrat drain	140.44	6.44		5.7	128.3	43.2	31.72
Elamom drain	148.47	8.07		6.2	129.2	44.5	29.61
Anatomical characters of petioles	Thickness of epidermis (μ)	Length of lacuna (μ)		Width of lacuna (μ)	Length of vascular bundle (μ)	Width of vascular bundle (μ)	
(Fresh water)	5.18	61.38		39.53	67.60	43.37	
Nashrat drain	4.97	54.91		32.49	73.73	39.72	
Elamom drain	5.13	52.49		28.32	50.81	35.32	

The microphotographs in Figure 3G–I show that the petiole consists of single epidermis layer and parenchyma cells contain vascular bundles. Each bundle was surrounded by bundle sheath of sclerenchyma cells. Epidermis thickness of petiole showed a reduction in plants grown in drainage water compared with plants grown in freshwater. Likewise, length and width of lacuna and vascular bundle of petiole (μ) showed reductions in plants grown in drainage water compared to those grown in freshwater (Figure 3G–I and Table 4).

3. Discussion

Large-scale utilization of water hyacinth for contaminated effluent purification is of great importance due to its high tolerance against biotic and abiotic stress conditions [29]. Although PTEs concentration in drainage water resources was relatively low, their mutual effects caused several deteriorations on molecular and anatomical characters of water hyacinth plants. These results are in agreement with [30] as water hyacinth plants can survive under a mixture of PTEs (Cd, Co, Cr, Cu, Mn, Ni, Pb, and Zn) up to 3 mg L^{-1} and under Pb^{2+} stress up to 100 mg L^{-1} . Concentrations of Ba and Sr were the highest among other PTEs ($0.053\text{--}0.1016 \text{ mg L}^{-1}$) and ($0.3437\text{--}1.107 \text{ mg L}^{-1}$), respectively. The translocation factor (TF) of the PTEs was > 1 suggesting the higher rhizofiltration efficiency of these metals by water hyacinth plants. According to Ma et al. [28], hyperaccumulating plants with $\text{TF} > 1$ are classified as high-efficient plants for PTEs translocation from roots into shoots. PTEs showed higher accumulation in roots compared to leaves. PTEs are mainly localized in vascular tissues and epidermal cells to mediate their translocation to other plant tissues [15]. Additionally, it may be localized as precipitates into metal binding compounds existed in cell walls (carbohydrates, cellulose, hemicellulose and lignin)

Results of PCA were performed by applying Varimax rotation with Kaiser normalization to assist the interpretation of PTEs concentration (Tables A1 and A2, and Figure A1, supporting information). PCA is commonly used in such studies to investigate the relationship between elements and their potential origins. Data as the different groups of elements that correlate together might have a similar common origin and similar behavior. The initial principal components (PC1 and PC2) explained about 87.5% of the variation (72.17 and 15.32%, respectively). In addition, PC1 and PC2 had the highest eigenvalues (11.55 and 2.45, respectively) as indicated in Table A1 in Appendix A, supporting information. Principle components 1 (PC1) showed high positive correlation and was loaded with Ba, Sr, Cu, Mn, Zn, Sb, and Ni, and it is suggested that these elements are derived from natural and anthropogenic origins. However, the rotated component matrix revealed that Fe, Cd, Cr, As, Al, Co, Ti, and Mo showed negative correlation and strongly correlated with principal component 2 (PC2), and these elements might be derived from industrial origins.

The obtained results illustrated the high tolerance of water hyacinth against PTEs stress. Genotoxicity of toxic elements can be assessed by molecular techniques such as Randomly Amplified Polymorphic DNA (RAPD). RAPD analysis showed generation of new DNA bands in plants grown in drainage water resources. These bands have not existed in plants grown in freshwater. Some of these bands have only existed in plants grown in the higher contaminated drainage water (Figure 1). [31] illustrated that DNA alterations detected by RAPD analysis offered a useful biomarker assay for the evaluation of genotoxic effects of PTEs in *Capsicum annum*. It was also reported that Cd has the capacity not only to cause morbidity to the exposed organisms but also has the potential to induce genotoxic adverse effects [32,33]. RAPD assay indicated damages and mutations in DNA induced directly and/or indirectly by the phytotoxic effect of copper [34]. RAPD assay also showed variations in band intensity, loss of typical bands and appearance of new bands suggesting several damages in DNA of barley seedling treated with Cd (30–120 mg/L⁻¹) [35].

The present study demonstrated the presence of 21 protein bands separated from leaves of water hyacinth plants grown in freshwater. Meanwhile, other plants grown in Elamom and Nashrat drains showed the presence of 22 and 23 protein bands, respectively. The protein profile of roots revealed detection of three protein bands of control plants. However, 16 protein bands were detected in roots of water hyacinth plants grown in drainage water resources. These findings are consistent with several reports confirming that PTEs exposure might cause complete elimination of some protein bands and creation of new ones [36,37]. Proteins are directly responsible for most biological processes in living cells. Therefore, it is necessary to conduct proteomic studies, which elucidate protein presence and role under certain environmental conditions [38]. It is well known that PTEs stress can activate a range of potential cellular mechanisms in plants, some of which being the mobilization of specific molecules such as stress proteins that play a very significant role in Cd detoxification and tolerance in plants [39,40]. The changes in protein banding patterns have been attributed to the occurrence of either gene mutation or induction of cytological aberrations. The absence of some bands might be due to the deletion of their corresponding genes.

Anatomically, water hyacinth has an epidermis layer, which is not covered by a cuticle or only covered with thin cuticle layer to support gas and nutrients absorption from surrounding water. The adverse effects of PTEs on cell growth and sizing caused a noticeable reduction in root diameter as well as thickness in cortex and vascular cylinder diameter in plants grown in drainage water. So far, no sufficient details are available regarding the anatomical responses of water hyacinth under PTEs stress. According to [41] no injurious effects on root anatomy of water hyacinth grown under the presence of As. Contrariwise, [42] reported that arsenic (As) stress caused several deteriorations in anatomical characters of water hyacinth leaves due to the reduction of cell size. The harmful effect of PTEs on the anatomical structure of water hyacinth may be attributed to the adverse effects on cell organelles and the nutrients imbalance in plant tissues [43,44]. The same harmful effects on anatomical structure were recorded under differs biotic and abiotic stresses in numerous plants [45–49]

4. Materials and Methods

4.1. Plant Material

A single clone from a population of water hyacinth covering large distribution area of Nile River (freshwater) was selected and surrounded by an opened cage to ensure the similar genetic background of experimented plants. Three groups of two weeks-old clones were transplanted in three different water resources: (i) freshwater source (Nile River) located at Desouk District, Kafr El-Sheikh Governorate (31°08′07.0″ N 30°38′01.6″ E), (ii) Elamom drain, Shubrakhit District, Beheira Governorate (31°01′40.2″ N 30°40′33.7″ E) and (iii) Nashart drain, Kafr El-Sheikh Governorate (31°05′51.3″ N 30°57′45.9″ E). The three homogenous clones were surrounded by a cages and left for three months until sexual reproduction and formation of homogenous clones comprising stolons, rhizomes, long pendant roots, and fruit clusters.

Samples were taken from each population for elemental, molecular, biochemical and anatomical analyses. Experimental procedures of all analyses were conducted at Genetics, Soil Sciences and Plant Pathology & Biotechnology Laboratory (PPBL) as well as EPCRS Excellence Center (certified according to ISO 17025, ISO 9001, ISO 14001 and OHSAS 18001), Department of Agricultural Botany, Faculty of Agriculture, Kafrelsheikh University, Kafr El-Sheikh, Egypt.

4.2. Elemental Analysis

Uniform-sized bottles were rinsed with the representative resources before water sampling. Water samples were taken at a depth of 10 cm from the surface of fresh and drainage water. Representative water samples were inserted into bottles leaving an appropriate head-space, and the bottles were tightly closed by caps to avoid potential contamination. Bottles were placed directly in the fridge until elemental analysis.

Water hyacinth plants were divided into roots and leaves in order to distinguish between the accumulation potentials of different plant organs. Plant samples (roots and leaves) were air-dried for a week, oven-dried at 70 °C until weight constant and mechanically ground to a fine powder using a stainless steel grinder. Plant samples were acid-digested for elemental determination of Ag, Al, As, Ba, Ca, Cd, Co, Cr, Cu, Fe, K, Mg, Mn, Mo, Na, Ni, P, Sb, Sr, Ti, V and Zn. Subsamples (1.0 g) of roots and leaves were digested using the mixture of concentrated nitric acid (HNO₃), hydrochloric acid (HCl) and 30% hydrogen peroxide (H₂O₂) [50,51].

Total elements concentration in water and plant samples was determined using Inductively Coupled Plasma Optical Emission Spectrometry (ICP-OES, model 5100, Agilent, Santa Clara, CA 95051, United States) at the Institute of Graduate Studies & Research, Alexandria University (accredited according to ISO/IEC 17025-2005). In the current study, bioaccumulation factor (BAF) and translocation factor (TF) for the most detected PTEs in water resources (Al, Ba, Cu, Mn, Sr, Ti, V, Zn) are given by:

$$BAF_{\text{roots}} = (C_{\text{root}})/(C_{\text{water}})$$

$$BAF_{\text{leaves}} = (C_{\text{leaves}})/(C_{\text{water}})$$

$$TF = (C_{\text{leaves}})/(C_{\text{root}})$$

where C_{water} , C_{root} , and C_{leaves} are PTEs concentrations in water (mg L⁻¹), leaves (mg kg⁻¹), and roots (mg kg⁻¹), respectively [28]. Quality control of data was performed with the use of repeat measurements for all obtained data. The mean relative standard deviation (RSD) was less than 5%. Principal component analysis (PCA) was performed using MVSP software ver 3.13 (Kovach Computing Services, Pentraeth, UK) [52] to assist the interpretation of PTEs concentration in water and plant samples.

4.3. Molecular Analysis

4.3.1. Total DNA Extraction

Total DNA was extracted from young leaves using the modified cetyl trimethylammonium bromide (CTAB) method [53] with some modifications. Leaves were wrapped in filter papers under hand pressure for five min to remove moisture, and 150 mg of samples were ground using pestle and mortar. Thereafter, 600 µL of preheated (65 °C) extraction buffer (2% CTAB, 20 mM EDTA, 100 mM Tris-HCl, 1.4 M NaCl, 2% polyvinylpyrrolidone, and 0.2% mercaptoethanol) were added. The mixture was transferred to a centrifuge tube (2 mL), incubated for 30 min in a 65 °C water bath, and samples were inverted every 5 min. 600 µL of chloroform-isoamyl alcohol (24:1) was added and mixed by inverting the tubes carefully for 8 times, and the mixture was centrifuged at 12,000 rpm for 10 min at room temperature. The supernatant was collected, carefully mixed with a two-third volume of ice-cold isopropanol, and the DNA samples were collected by centrifuging for 10 min. RNase (10 µg/mL) was added to the 50 µL of TE buffer (10 mM Tris and 0.1 mM EDTA) prior to dissolving the DNA to remove any RNA, and the mixture was incubated at 37 °C for 30 min. After incubation, 100 µL and 750 µL

volumes of 3.0 M sodium acetate and ice-cold absolute ethanol were added, respectively. The DNA was collected by high-speed centrifugation for 10 min, carefully washed with ice-cold absolute and 70% ethanol and centrifuged at 120000 rpm for 10 min. Finally, samples were dried at room temperature and dissolved in 50–100 µL of TE buffer. The quality and concentration of DNA were determined by a P330 photometer (EMPLEN, Munich, Germany).

4.3.2. RAPD—PCR

For DNA amplification, nine decamer RAPD primers (Operon technologies, CA, USA) were used (Table 1). PCR was performed as follows: initial denaturation at 94 °C for 5 min; followed by 35 cycles at 94 °C for 1 min, specific annealing temperature (T_a) for 30 s according the primer sequence and 72 °C for 3 min and the final extension step at 72 °C for 10 min. Amplification was carried out in MJ Mini Bio RAD, thermal cycler in 25 µL reaction volume containing the following reagents: 1.0 µL of dNTPs (10 mM), 1.0 µL of MgCl₂ (25 mM), 5 µL of 10 × buffer, 1.0 µL of primer (10 pmol), 1.0 µL of DNA (25 ng/µL), 0.3 µL of Taq polymerase (5u/µL) and 15.7 d.d. H₂O. The amplification products were resolved electrophoretically on 1.5% agarose gels in TAE buffer (40 mM Tris-acetate, 20 mM glacial acetic acid, 1 mM EDTA, pH 7) at 75 V. The gel was stained with ethidium bromide and then destained with tap water. Bands were detected on UV-trans-illuminator and photographed by a gel documentation system (UVITEC, city, UK).

4.3.3. Total Protein Extraction

Total proteins were extracted from water hyacinth leaves and roots. Briefly, approximately 0.5 g powder of fresh leaves and roots were homogenized by mechanical grinding and mixed well with 500 µL of the protein extraction buffer (62.5 mM Tris-HCl, pH 6.8, 2% SDS, 10% glycerol, 5% β-mercaptoethanol, 5 M Urea and 0.01% bromophenol blue) by vortexing. Protein extracts were centrifuged at 14,000 rpm for 10 min at 4 °C and separated by 12% (SDS-PAGE) according to [54]. Molecular weights of different bands were calibrated with a mixture of standard protein markers (Molecular Weight Marker, M. W. 14.000–66.000; Catalog No. SDS7, Sigma-Aldrich, Munich, Germany). The banding profile was stained by Coomassie blue dye then photographed and scored.

4.4. Anatomical Studies

Roots, leaves, and petioles of water hyacinth plants were sampled for anatomical characterization. Samples (0.5 cm length) were placed in FAA solution (killing and fixing), washed in 50% ethyl alcohol, and dehydrated in butyl alcohol series. Samples were impeded in paraffin wax (56–58 °C). Transverse sections (15 microns thick) were done with rotary microtome model 820, fixed with albumin, stained with a combination of safranin and light green, and finally fixed in Canada balsam [55]. The sections were investigated microscopically and photomicrographed (Leica, Wetzlar, Germany) [48,56,57].

5. Conclusions

Water hyacinth (*Eichhornia crassipes* (Mart.) Solms) is one of the most critical aquatic plants in Egypt and worldwide. Due to its hyper accumulating potentials of PTEs and its high resistance against biotic and abiotic stress conditions, water hyacinth has received significant attention to clean-up contaminated water effluents. However, research trials undertaken to improve adaptability of water hyacinth against PTEs stress are still very few. The novelty aspects of this research are to study molecular, biochemical and anatomical characters of water hyacinth subjected to PTEs stress. Although PTE's concentration in drainage water resources was relatively low, the hyperaccumulating potentials of water hyacinth maximized their concentration in plant tissues. Immobile PTEs (e.g., Al, As, Cd, Co, Cr, Cu, Fe, Mn, Mo, Ni, Sb, Ti, V, and Zn) showed higher accumulation in roots; however, mobile PTEs (e.g., Ba and Sr) exhibited higher accumulation in leaves. DNA alterations detected by RAPD analysis confirmed the genotoxic effects of PTEs. Protein profile alterations in electrophoretic profiles and banding patterns were observed on plants grown in drainage water resources, especially protein isolated from roots.

The ultrastructural analysis also showed several deteriorations on the anatomical structure of plants grown under PTEs stress. Further investigations should be undertaken to explore molecular and biochemical characters of plants grown under higher PTEs concentrations.

Author Contributions: F.S.M., A.E.-B., M.A.E.-E., M.M.A.-D., A.M. and K.A.A.A. performed the experiments, analyzed the data and wrote the manuscript. All authors have read and agreed to the published version of the manuscript.

Funding: This research was funded by Researchers Supporting Project number (RSP 2019/121), King Saud University, Riyadh, Saudi Arabia.

Acknowledgments: The authors would like to acknowledge King Saud University, Riyadh, Saudi Arabia and all members of PPB Lab and EPCRS Excellence Centre (Accredited according to ISO/17025, 9001, 14001 and OHSAS/18001), Department of Agricultural Botany, and all members of Genetics Department as well as Soil and Water Sciences Department, Faculty of Agriculture, Kafrelsheikh University, Kafr-Elsheikh, Egypt.

Conflicts of Interest: The authors declare no conflict of interest.

Appendix A

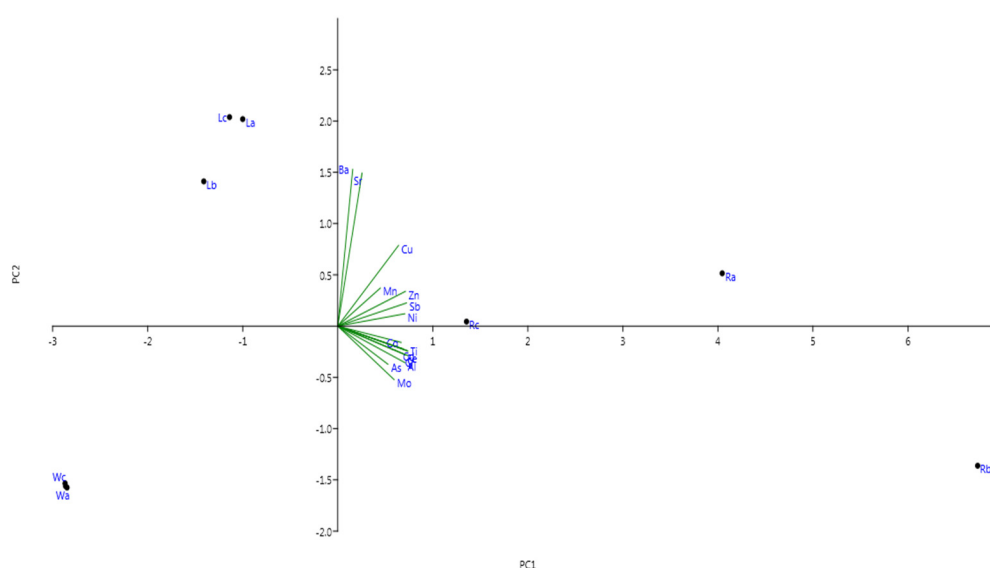


Figure A1. Biplot of principal component analysis (PC1 and PC2): Wa (water samples of Nile River), Wb (water samples of Nashart drain), Wc (water samples of Elamom drain), Ra (root samples of Nile River), Rb (root samples of Nashart drain), Rc (root samples of Elamom drain), La (leaf samples of Nile River), Lb (leaf samples of Nashart drain), and Lc (leaf samples of Elamom drain).

Table A1. Eigenvalues and variance percentage of PCA axes.

PC	Eigenvalue	% Variance
1	11.5466	72.166
2	2.45113	15.32
3	1.40781	8.7988
4	0.531421	3.3214
5	0.0542793	0.33925
6	0.00853064	0.053317
7	0.0001916	0.0011975
8	3.04211E-05	0.00019013

Table A2. Correlation values between PTEs and PCA axes.

	PC 1	PC 2	PC 3	PC 4	PC 5	PC 6	PC 7	PC 8
Fe	0.98706	-0.1504	0.055309	0.0015026	0.0029266	0.0031235	-0.0023979	0.00053446
Mn	0.6014	0.22974	-0.76378	-0.014811	0.039769	0.018957	0.0036508	0.00022535
Zn	0.95651	0.20998	0.16118	-0.063946	0.10446	0.0033057	-0.00071601	-0.0019101
Cu	85914	0.48739	0.090644	0.096371	0.049532	-0.066118	0.00059223	0.00026169
Cd	0.92614	-0.13717	-0.31575	-0.15343	0.011846	0.0078615	0.0012176	-0.0020004
Ni	0.94772	0.07455	-0.30531	0.025616	-0.035216	-0.033954	-0.00095696	0.0025461
V	0.98391	-0.17681	0.02068	0.0055642	0.0075217	0.011478	-0.002238	0.00037662
Cr	0.95266	-0.17325	0.20767	-0.13679	0.022293	0.0088111	-0.0041898	0.00020853
As	0.7089	-0.23022	0.33205	0.57763	-0.018081	0.014545	0.0019363	-0.00030312
Al	0.95133	-0.22099	0.18919	-0.10026	0.013453	0.0096037	-0.0040299	0.00037437
Co	0.8962	-0.098352	-0.35947	0.24016	0.0041221	0.015569	0.0024217	0.00016284
Sr	0.34233	0.92456	0.13955	-0.057268	-0.061917	0.037568	-0.0010578	0.0022479
Ti	0.98866	-0.14892	-0.0029339	-0.015794	0.0059686	0.0081479	-0.0022106	0.00049535
Sb	0.97084	0.13976	-0.0079054	-0.078706	-0.17742	-0.014078	0.00039766	-0.002582
Mo	0.79596	-0.32305	0.44719	-0.24897	0.00016716	0.001651	0.010578	0.0013171
Ba	0.21113	0.9466	0.23648	0.042286	0.03895	0.011402	0.0016721	-0.001319

Table A3. SDS-PAGE banding patterns of total protein isolated from leaves and roots of water hyacinth grown in fresh and drainage water resources.

Band No	(KDa)	Roots			Leaves			(KDa)	Band No.
		Elamom Drain	Nashrat Drain	Fresh Water	Elamom Drain	Nashrat Drain	Fresh Water		
1	46	++	+	-	++++	++++	++	66	1
2	45.7	+	+	-	++++	++++	++	65.8	2
3	45	+	+	-	+	-	-	64.3	3
4	44.4	+	+	-	+	+	+	60.2	4
5	36	++	++	-	+	+	-	50.5	5
6	29	++	+	-	++	++	++	47	6
7	28.4	++	+	-	+++	+++	+++	45	7
8	28	+	-	-	+++	+++	+++	44.6	8
9	20.6	++	++	+	+++++	+++++	+++++	36	9
10	18.1	+	+	+	++	++	++	29	10
11	17.6	+	+	-	++	++	++	28.7	11
12	16.3	++	++	+	++	++	++	27.6	12
13	15	+	+	-	++	++	++	26.4	13
14	14	+	+	-	++	++	++	18.2	14
15	13.9	+	+	-	++	++	++	17.3	15
					++	++	++	16.5	16
					+	+	+	15.2	17
					+	+	+	14.9	18
					+++	+++	+++	14.8	19
					+++	+++	+++	14.7	20
					+++	+++	+++	14	21
					+	+	+	13.8	22
					+	+	+	13.5	23

Note: +++++→very strong; +++→strong; ++→intermediate; +→weak; -→absent.

References

- Binet, M.T.; Adams, M.S.; Gissi, F.; Golding, L.A.; Schlekat, C.E.; Garman, E.R.; Merrington, G.; Stauber, J.L. Toxicity of nickel to tropical freshwater and sediment biota: A critical literature review and gap analysis. *Environ. Toxicol. Chem.* **2018**, *37*, 293–317. [[CrossRef](#)]
- Fang, J.; Gao, B.; Mosa, A.; Zhan, L. Chemical activation of hickory and peanut hull hydrochars for removal of lead and methylene blue from aqueous solutions. *Chem. Speciat. Bioavailab.* **2017**, *29*, 197–204. [[CrossRef](#)]
- Song, J.; He, Q.; Hu, X.; Zhang, W.; Wang, C.; Chen, R.; Wang, H.; Mosa, A. Highly efficient removal of Cr (VI) and Cu (II) by biochar derived from *Artemisia argyi* stem. *Environ. Sci. Pollut. Res.* **2019**, *26*, 13221–13234. [[CrossRef](#)] [[PubMed](#)]
- Fu, L.; Lu, X.; Niu, K.; Tan, J.; Chen, J. Bioaccumulation and human health implications of essential and toxic metals in freshwater products of Northeast China. *Sci. Total Environ.* **2019**, *673*, 768–776. [[CrossRef](#)] [[PubMed](#)]
- Järup, L. Hazards of heavy metal contamination. *Br. Med. Bull.* **2003**, *68*, 167–182. [[CrossRef](#)]
- Abdullah, N.; Yusof, N.; Lau, W.J.; Jaafar, J.; Ismail, A.F. Recent trends of heavy metal removal from water/wastewater by membrane technologies. *J. Ind. Eng. Chem.* **2019**, *76*, 17–38. [[CrossRef](#)]

7. Berni, R.; Luyckx, M.; Xu, X.; Legay, S.; Sergeant, K.; Hausman, J.-F.; Lutts, S.; Cai, G.; Guerriero, G. Reactive oxygen species and heavy metal stress in plants: Impact on the cell wall and secondary metabolism. *Environ. Expe. Bot.* **2019**, *161*, 98–106. [[CrossRef](#)]
8. Maleki, M.; Ghorbanpour, M.; Kariman, K. Physiological and antioxidative responses of medicinal plants exposed to heavy metals stress. *Plant Gene* **2017**, *11*, 247–254. [[CrossRef](#)]
9. Soliman, M.; Alhaithloul, H.A.; Hakeem, K.R.; Alharbi, B.M.; El-Esawi, M.; Elkelish, A. Exogenous Nitric Oxide Mitigates Nickel-Induced Oxidative Damage in Eggplant by Upregulating Antioxidants, Osmolyte Metabolism, and Glyoxalase Systems. *Plants* **2019**, *8*, 562. [[CrossRef](#)]
10. Elkelish, A.A.; Alhaithloul, H.A.S.; Qari, S.H.; Soliman, M.H.; Hasanuzzaman, M. Pretreatment with *Trichoderma harzianum* alleviates waterlogging-induced growth alterations in tomato seedlings by modulating physiological, biochemical, and molecular mechanisms. *Environ. Expe. Bot.* **2020**, *171*, 103946. [[CrossRef](#)]
11. Jalmi, S.K.; Bhagat, P.K.; Verma, D.; Noryang, S.; Tayyeba, S.; Singh, K.; Sharma, D.; Sinha, A.K. Traversing the links between heavy metal stress and plant signaling. *Front. Plant Sci.* **2018**, *9*, 12. [[CrossRef](#)] [[PubMed](#)]
12. Siddiqui, S. DNA damage in Cicer plant grown on soil polluted with heavy metals. *J. King Saud Univ. Sci.* **2015**, *27*, 217–223. [[CrossRef](#)]
13. Zhang, X.; Li, M.; Yang, H.; Li, X.; Cui, Z. Physiological responses of *Suaeda glauca* and *Arabidopsis thaliana* in phytoremediation of heavy metals. *J. Environ. Manag.* **2018**, *223*, 132–139. [[CrossRef](#)] [[PubMed](#)]
14. Mosa, A.; El-Ghamry, A.; Trüby, P.; Omar, M.; Gao, B.; Elnaggar, A.; Li, Y. Chemo-mechanical modification of cottonwood for Pb²⁺ removal from aqueous solutions: Sorption mechanisms and potential application as biofilter in drip-irrigation. *Chemosphere* **2016**, *161*, 1–9. [[CrossRef](#)]
15. El-Banna, M.F.; Mosa, A.; Gao, B.; Yin, X.; Wang, H.; Ahmad, Z. Scavenging effect of oxidized biochar against the phytotoxicity of lead ions on hydroponically grown chicory: An anatomical and ultrastructural investigation. *Ecotoxicol. Environ. Saf.* **2019**, *170*, 363–374. [[CrossRef](#)]
16. Minkina, T.; Fedorenko, G.; Nevidomskaya, D.; Fedorenko, A.; Chaplygin, V.; Mandzhieva, S. Morphological and anatomical changes of *Phragmites australis* Cav. due to the uptake and accumulation of heavy metals from polluted soils. *Sci. Total Environ.* **2018**, *636*, 392–401. [[CrossRef](#)]
17. Baruah, S.; Bora, M.S.; Sharma, P.; Deb, P.; Sarma, K.P. Understanding of the distribution, translocation, bioaccumulation, and ultrastructural changes of *Monochoria hastata* plant exposed to cadmium. *Water Air Soil Pollut.* **2017**, *228*, 17. [[CrossRef](#)]
18. Ali, H.; Khan, E.; Sajad, M.A. Phytoremediation of heavy metals—Concepts and applications. *Chemosphere* **2013**, *91*, 869–881. [[CrossRef](#)]
19. Rezaia, S.; Ponraj, M.; Din, M.F.M.; Songip, A.R.; Sairan, F.M.; Chelliapan, S. The diverse applications of water hyacinth with main focus on sustainable energy and production for new era: An overview. *Renew. Sustain. Energy Rev.* **2015**, *41*, 943–954. [[CrossRef](#)]
20. Mosa, A.; El-Ghamry, A.; Tolba, M. Functionalized biochar derived from heavy metal rich feedstock: Phosphate recovery and reusing the exhausted biochar as an enriched soil amendment. *Chemosphere* **2018**, *198*, 351–363. [[CrossRef](#)]
21. Rezaia, S.; Ponraj, M.; Talaiekhosani, A.; Mohamad, S.E.; Din, M.F.M.; Taib, S.M.; Sabbagh, F.; Sairan, F.M. Perspectives of phytoremediation using water hyacinth for removal of heavy metals, organic and inorganic pollutants in wastewater. *J. Environ. Manag.* **2015**, *163*, 125–133. [[CrossRef](#)] [[PubMed](#)]
22. Chunkao, K.; Nimpee, C.; Duangmal, K. The King’s initiatives using water hyacinth to remove heavy metals and plant nutrients from wastewater through Bueng Makkasan in Bangkok, Thailand. *Ecol. Eng.* **2012**, *39*, 40–52. [[CrossRef](#)]
23. Smolyakov, B.S. Uptake of Zn, Cu, Pb, and Cd by water hyacinth in the initial stage of water system remediation. *Appl. Geochem.* **2012**, *27*, 1214–1219. [[CrossRef](#)]
24. Saha, P.; Shinde, O.; Sarkar, S. Phytoremediation of industrial mines wastewater using water hyacinth. *Int. J. Phytoremed.* **2017**, *19*, 87–96. [[CrossRef](#)]
25. Thapa, G.; Das, D.; Gunupuru, L.R.; Tang, B. Endurance assessment of *Eichhornia crassipes* (Mart.) Solms, in heavy metal contaminated site—A case study. *Cogent Environ. Sci.* **2016**, *2*, 1215280. [[CrossRef](#)]
26. Hussain, M.S.; Jamil, K. Bioaccumulation of heavy metal ions and their effect on certain biochemical parameters of water hyacinth weevil *Neochetina eichhorniae* (Warner). *J. Environ. Sci. Health Part B* **1989**, *24*, 251–264. [[CrossRef](#)]

27. Elkelish, A.A.; Alnusaire, T.S.; Soliman, M.H.; Gowayed, S.; Senousy, H.H.; Fahad, S. Calcium availability regulates antioxidant system, physio-biochemical activities and alleviates salinity stress mediated oxidative damage in soybean seedlings. *J. Appl. Bot. Food Qual.* **2019**, *92*, 258–266.
28. Ma, L.Q.; Komar, K.M.; Tu, C.; Zhang, W.; Cai, Y.; Kennelley, E.D. A fern that hyperaccumulates arsenic. *Nature* **2001**, *409*, 579. [[CrossRef](#)]
29. Wang, Z.; Zhang, Z.; Zhang, J.; Zhang, Y.; Liu, H.; Yan, S. Large-scale utilization of water hyacinth for nutrient removal in Lake Dianchi in China: The effects on the water quality, macrozoobenthos and zooplankton. *Chemosphere* **2012**, *89*, 1255–1261. [[CrossRef](#)]
30. Soltan, M.E.; Rashed, M.N. Laboratory study on the survival of water hyacinth under several conditions of heavy metal concentrations. *Adv. Environ. Res.* **2003**, *7*, 321–334. [[CrossRef](#)]
31. Aslam, R.; Ansari, M.Y.K.; Choudhary, S.; Bhat, T.M.; Jahan, N. Genotoxic effects of heavy metal cadmium on growth, biochemical, cyto-physiological parameters and detection of DNA polymorphism by RAPD in *Capsicum annum* L.—An important spice crop of India. *Saudi J. Biol. Sci.* **2014**, *21*, 465–472. [[CrossRef](#)] [[PubMed](#)]
32. Cimino, M.C. Comparative overview of current international strategies and guidelines for genetic toxicology testing for regulatory purposes. *Environ. Mol. Mutagen.* **2006**, *47*, 362–390. [[CrossRef](#)]
33. Azimi, A.; Shahriari, F.; Fotovat, A.; Qale, R.K.; Agje, K.H. Investigation of DNA changes in wheat (*Triticum aestivum* L.) induced by cadmium using random amplified polymorphic DNA (RAPD) analysis. *Afr. J. Biotechnol.* **2013**, *12*. [[CrossRef](#)]
34. Körpe, D.A.; Aras, S. Evaluation of copper-induced stress on eggplant (*Solanum melongena* L.) seedlings at the molecular and population levels by use of various biomarkers. *Mutat. Res. Genet. Toxicol. Environ. Mutagen.* **2011**, *719*, 29–34. [[CrossRef](#)] [[PubMed](#)]
35. Liu, W.; Yang, Y.S.; Li, P.J.; Zhou, Q.X.; Xie, L.J.a.; Han, Y.P. Risk assessment of cadmium-contaminated soil on plant DNA damage using RAPD and physiological indices. *J. Hazard. Mater.* **2009**, *161*, 878–883. [[CrossRef](#)] [[PubMed](#)]
36. Labra, M.; Gianazza, E.; Waitt, R.; Eberini, I.; Sozzi, A.; Regondi, S.; Grassi, F.; Agradi, E. Zea mays L. protein changes in response to potassium dichromate treatments. *Chemosphere* **2006**, *62*, 1234–1244. [[CrossRef](#)] [[PubMed](#)]
37. Novo, M.T.M.; da Silva, A.C.; Moreto, R.; Cabral, P.C.P.; Costacurta, A.; Garcia, O.; Ottoboni, L.M.M. Thiobacillus ferrooxidans response to copper and other heavy metals: Growth, protein synthesis and protein phosphorylation. *Antonie Van Leeuwenhoek* **2000**, *77*, 187–195. [[CrossRef](#)]
38. Porubleva, L.; Chitnis, P.R. *Proteomics: A Powerful Tool in the Post-Genomic Era*; NISCAIR-CSIR: New Delhi, India, 2000.
39. Delhaize, E.; Robinson, N.J.; Jackson, P.J. Effects of cadmium on gene expression in cadmium-tolerant and cadmium-sensitive *Datura innoxia* cells. *Plant Mol. Biol.* **1989**, *12*, 487–497. [[CrossRef](#)]
40. Di Toppi, L.S.; Gabbriellini, R. Response to cadmium in higher plants. *Environ. Exp. Bot.* **1999**, *41*, 105–130. [[CrossRef](#)]
41. Pereira, F.J.; Castro, E.M.; Oliveira, C.; Pires, M.F.; Pasqual, M. Anatomical and physiological mechanisms of water hyacinth plants to arsenic contamination tolerance. *Planta Daninha* **2011**, *29*, 259–267. [[CrossRef](#)]
42. Qaisar, M.; Ping, Z.; Rehan, S.M.; Rashid, A.M.; Yousaf, H. Anatomical studies on water hyacinth (*Eichhornia crassipes* (Mart.) Solms) under the influence of textile wastewater. *J. Zhejiang Univ. Sci. B* **2005**, *6*, 991–998.
43. Sooknah, R.D.; Wilkie, A.C. Nutrient removal by floating aquatic macrophytes cultured in anaerobically digested flushed dairy manure wastewater. *Ecol. Eng.* **2004**, *22*, 27–42. [[CrossRef](#)]
44. Gratão, P.L.; Monteiro, C.C.; Rossi, M.L.; Martinelli, A.P.; Peres, L.E.P.; Medici, L.O.; Lea, P.J.; Azevedo, R.A. Differential ultrastructural changes in tomato hormonal mutants exposed to cadmium. *Environ. Exp. Bot.* **2009**, *67*, 387–394. [[CrossRef](#)]
45. Abdelaal, K.H.A.A.; Hafez, Y.M.; Badr, M.M.; Youseef, W.A.; Esmail, S.M. Biochemical, histological and molecular changes in susceptible and resistant wheat cultivars inoculated with stripe rust fungus *Puccinia striiformis* f. sp. tritici. *Egypt. J. Biol. Pest. Control.* **2014**, *24*, 421–429.
46. Abdelaal, K.H.A.A. Effect of salicylic acid and abscisic acid on morpho-physiological and anatomical characters of faba bean plants (*Vicia faba* L.) under drought stress. *J. Plant Prod.* **2015**, *6*, 1771–1788. [[CrossRef](#)]
47. Helaly, M.; Mohammed, Z.; El-Shaery, N.; Abdelaal, K.H.A.A.; Nofal, I. Cucumber grafting onto pumpkin can represent an interesting tool to minimize salinity stress. Physiological and anatomical studies. *Middle East J. Agric. Res.* **2017**, *6*, 953–975.
48. Abdelaal, K.H.A.A.; Reda, O.I.; Yaser, H.M.; Esmail, S.M.; El Sabagh, A. Anatomical, biochemical and physiological changes in some Egyptian wheat cultivars inoculated with *Puccinia graminis* f. sp. tritici. *Fresenius Environ. Bull.* **2018**, *27*, 296–305.

49. Abdelaal, K.H.A.A.; El Menofy, E.M.; Nessem, A.A.; Elhaak, M.A. The allelopathy potential and Glyphosate influence on anatomical features of Egyptian clover plant (*Trifolium alexandrinum* L.) infested with dodder weed (*Cuscuta campestris* L.). *Freesnius Environ. Bull.* **2019**, *28*, 1273–1280.
50. Huang, C.Y.L.; Schulte, E.E. Digestion of plant tissue for analysis by ICP emission spectroscopy. *Commun. Soil Sci. Plant Anal.* **1985**, *16*, 943–958. [[CrossRef](#)]
51. Jones, J.B., Jr. *Laboratory Guide for Conducting Soil Tests and Plant Analysis*; CRC Press: Boca Raton, FL, USA, 2001.
52. Kovach, W.L. *A Multivariate Statistical Package for Windows, ver 3.1*; Kovach Computing Services: Pentraeth, UK, 1999.
53. Doyle, J.J.; Doyle, J.L. Isolation of plant DNA from fresh tissue. *Focus* **1990**, *12*, 39–40.
54. Laemmli, U.K. Cleavage of structural proteins during the assembly of the head of bacteriophage T4. *Nature* **1970**, *227*, 680–685. [[CrossRef](#)] [[PubMed](#)]
55. Nassar, M.A.; El-Sahhar, K.F. *Botanical Preparations and Microscopy (Microtechnique)*; Academic Bookshop: Giza, Egypt, 1998; p. 219.
56. Omara, R.I.; Abdelaal, K.A.A. Biochemical, histopathological and genetic analysis associated with leaf rust infection in wheat plants (*Triticum aestivum* L.). *Physiol. Mol. Plant Pathol.* **2018**, *104*, 48–57. [[CrossRef](#)]
57. Esmail, S.M.; Omara, R.I.; Abdelaal, K.A.A.; Hafez, M. Histological and biochemical aspects of compatible and incompatible wheat-*Puccinia striiformis* interactions. *Physiol. Mol. Plant Pathol.* **2019**, *106*, 120–128. [[CrossRef](#)]



© 2020 by the authors. Licensee MDPI, Basel, Switzerland. This article is an open access article distributed under the terms and conditions of the Creative Commons Attribution (CC BY) license (<http://creativecommons.org/licenses/by/4.0/>).